

Time variations of the narrow Fe II and H I spectral emission lines from the close vicinity of η Carinae during the spectral event of 2003[★]

H. Hartman¹, A. Damineli², S. Johansson¹, and V. S. Letokhov^{3,1}

¹ Lund Observatory, Lund University, PO Box 43, 22100, Lund, Sweden
e-mail: henrik.hartman@astro.lu.se

² Instituto de Astronomia, Geofísica e Ciências Atmosféricas, University of Sao Paulo, Rua do Matao 1226, 05508-900 Sao Paulo, Brazil

³ Institute of Spectroscopy, Russian Academy of Sciences, Troitsk, Moscow region, 142190, Russia

Received 7 February 2005 / Accepted 9 March 2005

Abstract. The spectrum of Eta Carinae and its ejecta shows slow variations over a period of 5.5 years. However, the spectrum changes drastically on a time scale of days once every period called the “spectral event”. We report on variations in the narrow emission line spectrum of gas condensations (the Weigelt blobs) close to the central star during a spectral event. The rapid changes in the stellar radiation field illuminating the blobs make the blobs a natural astrophysical laboratory to study atomic photoprocesses. The different responses of the H I Paschen lines, fluorescent \langle Fe II \rangle lines and forbidden [Fe II] lines allow us to identify the processes and estimate physical conditions in the blobs. This paper is based on observations from the Pico dos Dias Observatory (LNA/Brazil) during the previous event in June 2003.

Key words. atomic processes – radiation mechanisms: non-thermal – ISM: H II regions – stars: individual: Eta Carinae

1. Introduction

A general description of Eta Carinae and its nebulosities is given by Davidson and Humphreys (1997). During the last decade more detailed information about the complex object has been obtained thanks to high-resolution spatial and spectral observations performed with the Hubble Space Telescope (Gull et al. 2001) and the VLT/UVES instrument (Weis et al. 2005; Stahl et al. 2005). The observational data have shown that Eta Carinae and its close environment contain a number of unique spectroscopic challenges formulated by Davidson (2001).

Eta Carinae is one of the most luminous and massive stars in the Galaxy, and the site of huge non-thermal stellar eruptions as well as the source of radiation with very different properties. Wide Doppler-shifted spectral lines originate from fast moving ejecta in the Homunculus, thereby being a source of information about the kinematics of the expanding asymmetrical hollow lobes (Smith et al. 2004). Similar information is obtained from several velocity systems detected by numerous blue-shifted absorption lines of many elements (Gull et al. 2005). A forest of narrow spectral emission lines originate from dense slowly-moving ejecta near Eta Carinae (Davidson et al. 1995), which were detected and resolved as a few objects (the Weigelt blobs B, C, D) by Weigelt & Ebersberger (1986) using

speckle-interferometry. A two-zone photoionization model of the Weigelt blobs was developed by Johansson and Letokhov in 2001–2004, which provides a natural explanation of the origin of the narrow emission lines from a H I zone and the wider lines from a H II zone inside the blobs. This photoionization model is also quite useful for the explanation of a time variation observed in the narrow Fe II and H I spectral lines during the spectroscopic event in 2003, which is subject of the present paper. The densities and temperatures used in our model of the blobs are similar to those derived by Verner et al. (2002).

The neighborhood of the massive star Eta Carinae is for many reasons a giant natural space laboratory for atomic astrophysics. Firstly, in the immediate vicinity of the central source we find the Weigelt blobs B, C, D, having a hydrogen concentration of the order of 10^8 cm^{-3} (Davidson & Humphreys 1997). At such a low hydrogen concentration, collisional processes occur on a time scale much larger than 1 s. For this reason, the radiative relaxation of excited atoms and ions occurs under collision-free conditions, which somewhat facilitates the interpretation of the complicated observed spectra.

Secondly, the Weigelt blobs are located at angular distances of the order of 0.1–0.2 arcsec from the central star, i.e., at around 300 stellar radii (r_s), where $r_s = 3 \times 10^{13} \text{ cm}$ (van Boekel et al. 2003). The small distance provides for a strong photoionization of the blobs and the stellar wind by the Lyman continuum radiation, Ly_c from the photosphere of Eta Carinae.

[★] Based on data collected at the Pico dos Dias Observatory (LNA-MCT).

A substantial proportion of the absorbed radiation is converted into H Ly α radiation by photorecombination. Thus, the close ejecta of Eta Carinae are irradiated by intense Ly α radiation corresponding to an effective spectral temperature above 10 000 K (Johansson & Letokhov 2004a).

Thirdly, the coincidence between the wide H Ly α spectral line and a dozen of Fe II absorption lines (Brown et al. 1979; Johansson & Jordan 1984) gives rise to a number of fluorescence (Fe II) lines from highly excited states. Especially conspicuous among them are the abnormally bright 2507/09-Å UV lines of Fe II (Johansson & Hamann 1993). The fluorescence lines have a small spectral width, since they originate in the relatively cold HI regions of the partially ionized Weigelt blobs (Johansson & Zethson 1999; Johansson & Letokhov 2001). The first indication that the narrow Fe II lines actually are formed in the Weigelt blobs was based on observations with the FOS instrument onboard the Hubble Space Telescope (Davidson et al. 1995) and later confirmed by numerous observations of Eta Carinae with GHRS and STIS (Davidson et al. 1997; Gull et al. 1999).

In the fourth place, when attempting to explain the origin of the abnormally bright 2507/09 Å lines from a detailed analysis of the Fe II spectrum and the radiative relaxation pathways of high-lying, H Ly α -pumped Fe II levels, the idea of stimulated emission of radiation (the astrophysical laser) in transitions from long-lived (pseudo-metastable) Fe II states has been proposed (Johansson & Letokhov 2002). The stimulated emission yields a purely radiative cycle of Fe II in a four-level scheme pumped by intense H Ly α radiation. The closed cycle gives rise to the intense UV spontaneous emission lines of Fe II (Johansson & Letokhov 2003, 2004b).

Finally, as a fifth point, the discovery by Damineli (1996) of the periodic (5.5 years) reduction of the intensity of photospheric He lines for a few months, called “the spectroscopic event”, offers a unique possibility to use time probing of the photophysical processes taking place in the blobs. The periodicity led Damineli et al. (1997) to propose a binary system composed by evolved massive stars. The expected wind-wind collision is revealed by an X-ray source, which is variable and whose hard X-rays is deeply absorbed (Pittard & Corcoran 2002). The detection of phase locked He II 4686 Å emission is an indirect evidence that the secondary star is much hotter than the primary and is the source of ionization for the high excitation lines seen in the Weigelt blobs (Steiner & Damineli 2004). It is especially valuable that the relatively small distance (7500 l.y.) to Eta Carinae makes it possible to observe the spectral response of the blobs to such a periodic change in the intensity of the photoionizing radiation from Eta Carinae with a high spatial (angular) and spectral resolution by means of the *HST*/STIS facility (Gull et al. 2001).

This paper presents the result of ground-based spectroscopic observations of narrow Fe II and H Paschen lines from the Weigelt blobs of Eta Carinae made during the spectral event of 2003. We selected these Fe II lines, which are narrow relative to stellar wind lines, and emitted by the cool (HI) zone, and also narrow Paschen lines from the hot HII zone of the slow-moving blobs. First (Sect. 2) we briefly describe the basic photoprocesses occurring in the Weigelt blobs receiving

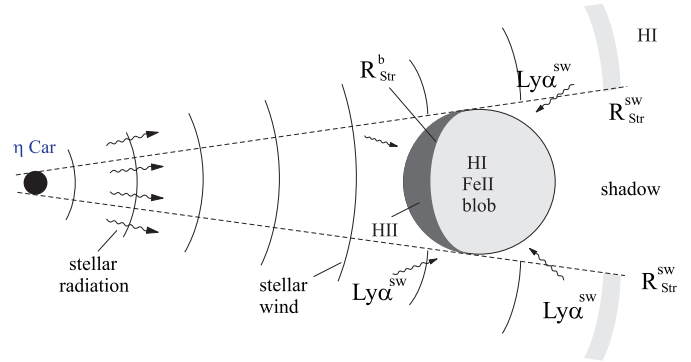


Fig. 1. A sketch of the formation of fluorescent and forbidden spectral lines in a Weigelt blob with the H II and HI zones irradiated by Ly α ^{sw} from the stellar wind ($R_{\text{Str}}^{\text{b}}$ and $R_{\text{Str}}^{\text{sw}}$ are the Strömgren boundaries in the blob and stellar wind, respectively).

radiation from the central source, a primary and a secondary star, and also the intense Ly α radiation from the stellar wind. The observations are described in Sect. 3. In the subsequent sections, we describe and interpret the temporal behavior of the intensity of: the Paschen lines (Sect. 4), the fluorescent ⟨Fe II⟩ lines, including the Fe II fluorescent probing of the width of the wind component of Ly α (Sect. 5), and forbidden [Fe II] lines from low-lying metastable states (Sect. 6). In the conclusion (Sect. 7), we discuss the validity of our simple model for the basic photoprocesses taking place in the Weigelt blobs (Sect. 2) on the basis of the observational data presented.

2. Basic photoprocesses occurring in the weigelt blobs

Before discussing the observational data available, it seems worthwhile to present a general picture of the photoprocesses taking place in the Weigelt blobs. This picture has emerged during the course of investigations that are aimed at explaining the abnormally bright 2507/09 Å spectral lines of Fe II (Johansson & Letokhov 2002, 2004a,b).

Figure 1 presents a simplified geometry of an average blob (blob B, for example) surrounded by the stellar wind of Eta Carinae. Consider the case where the Strömgren boundary for the stellar wind, $R_{\text{Str}}^{\text{sw}}$, is located behind the blob, i.e., $R_{\text{Str}}^{\text{sw}} > R_{\text{b}}$, where R_{b} is the distance between the blob and the central source. In that case, the ionizing radiation from the central source reaches the surface of the blob and photoionizes its front part. Thus, the Strömgren boundary for the blob, $R_{\text{Str}}^{\text{b}}$, intersects the blob, dividing it into a hot (HII) and a cold (HI) zone. The Ly α radiation generated in the HII region of the blob and in the stellar wind irradiates the blob on all sides. The Ly α radiation from the stellar wind has a broad spectrum determined by the terminal velocity $v_{\text{t}} \simeq 650 \text{ km s}^{-1}$: $\Delta v_{\text{sw}} = 2(v_{\text{t}}/c)v_0$, where v_0 is the central frequency of the Ly α radiation. The spectrum of the Ly α radiation incident on the slow-moving blob from the stellar wind can be shifted either toward the blue or toward the red, depending on the direction of the radiation: when the blob is irradiated from behind (in opposite direction of its movement), the radiation spectrum is red-shifted, and when it is

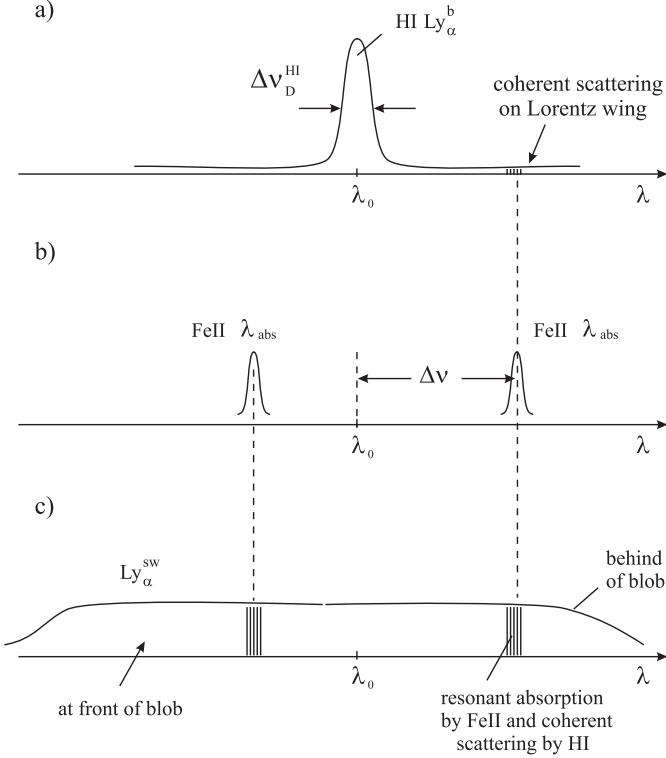


Fig. 2. Illustration of the mutual positions of spectral lines: **a)** $\text{Ly}\alpha^b$ in the blob; **b)** Fe II absorption lines; **c)** wide $\text{Ly}\alpha^{\text{sw}}$ from the stellar wind.

irradiated in the same direction as it moves, the spectrum is blue-shifted (Figs. 1 and 2).

The Fe^+ ions are formed both in the hot (HII) and in the cold (HI) zones of the blob, since the optical density of the Fe I-ionizing radiation ($919 \text{ \AA} < \lambda_{\text{ion}} < 1520 \text{ \AA}$) is not very high. In other words, the Fe I photoionization rate is much higher than the Fe II-electron recombination rate, $W_{\text{ph}} \gg W_{\text{rec}}$. In fact, the mean Fe I photoionization cross section $\langle \sigma_{\text{ph}} \rangle \approx 10^{-18} \text{ cm}^2$, whereas the Fe II recombination coefficient $\alpha_{\text{rec}} \approx 10^{-11} \text{ cm}^3 \text{ s}^{-1}$ (Bautista & Pradhan 1998). With an effective temperature $T \approx 30000 \text{ K}$ of the ionizing radiation from the central source, the ionizing radiation flux in the frequency region corresponding to the 5 eV gap between the ionization potentials of Fe I and HI is $\Phi_{\text{phr}} \approx 5 \times 10^{23} \text{ photons/cm}^2 \text{ s}\cdot\text{sr}$. Therefore, the photoionization rate of Fe I is

$$W_{\text{ph}} = \langle \sigma_{\text{ph}} \rangle \Phi_{\text{ph}} \Omega \approx 0.5\text{--}5 \text{ s}^{-1}, \quad (1)$$

where $\Omega = \frac{1}{4}(r_s/R_b)^2 \approx 10^{-6}\text{--}10^{-5}$ is the dilution factor, and R_b is the distance between the blob and the central source. At the same time, the Fe II + e recombination rate is

$$W_{\text{rec}} \approx \alpha_{\text{rec}} \cdot n_e \approx 10^{-8}\text{--}10^{-7} \text{ s}^{-1} \approx 10^{-3} \text{ to } 10^{-2} \text{ day}^{-1}, \quad (2)$$

where it is assumed that the electron density in the HI zone is governed mainly by the photoionization of Fe I, i.e. $n_e \approx N(\text{Fe II}) = 10^{-4}N_{\text{H}} \approx 10^3\text{--}10^4 \text{ cm}^{-3}$ for $N_{\text{H}} \approx 10^7\text{--}10^8 \text{ cm}^{-3}$.

The $\text{Ly}\alpha$ radiation responsible for the photoselective excitation of Fe II can stem from two sources. First, an intense $\text{Ly}\alpha$ radiation generated in the HII zone of the blob enters its HI

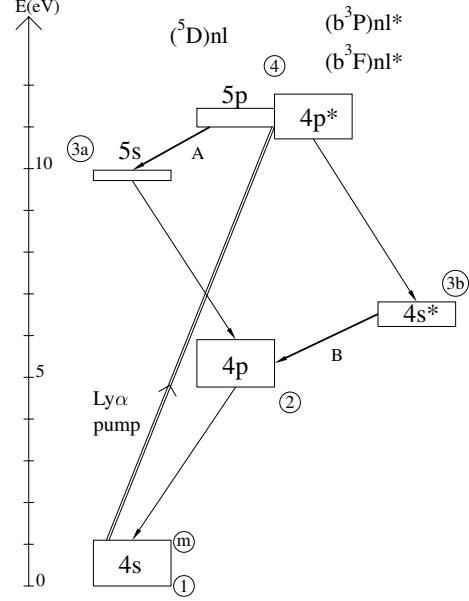


Fig. 3. Partial energy level diagram of Fe II, including only the set of levels discussed in the present paper. The lines of relevance are marked with A and B. These are primary and secondary decays, respectively, of the H $\text{Ly}\alpha$ pumped levels. The circled numbers are introduced to make the discussion in the text easier to follow.

zone. However, the penetration depth of this spectrally narrow radiation is restricted by the high optical density of absorption in the $\text{Ly}\alpha$ transition, and the significant ($\pm 2.5 \text{ \AA}$) detuning of the Fe II absorption lines relative to $\text{Ly}\alpha$. This matter was considered by Klimov et al. (2002). The situation is more clear when one considers the $\text{Ly}\alpha$ radiation generated in the stellar wind in the geometry shown in Fig. 1. This radiation has a broad spectrum for the slow-moving HI and Fe II zones in the blob. The Fe II ion can undergo photoselective excitation when it is in exact resonance with the red-shifted component of the $\text{Ly}\alpha$ radiation from the stellar wind (Fig. 2).

Next question concerns the optical depth in the Fe II absorption line from a low-lying metastable state “ m ” (see Fig. 3) to the high-lying state 4 that leads to a chain of fluorescence transitions $4 \rightarrow 3 \rightarrow 2 \rightarrow \dots$ and so on. The optical depth τ_{m4} (Fe II) can be estimated by the standard expression

$$\tau_{m4}(\text{Fe II}) = \sigma_{m4} N_m^{\text{Fe II}} r_b, \quad (3)$$

where σ_{m4} is the absorption cross section in the $m \rightarrow 4$ transition,

$$\sigma_{m4} = \frac{\lambda_{m4}^2}{2\pi} \frac{A_{4m}}{2\pi \Delta v_D^{m4}}. \quad (4)$$

$N_m^{\text{Fe II}}$ is the population of the low-lying initial state “ m ” (one of about 60 metastable states), r_b is the radius of the spherical blob, A_{4m} is the Einstein coefficient, and Δv_D^{m4} is the Doppler width of the Fe II absorption line. Adopting the following numerical data: $A_{4m} \approx 10^8 \text{ s}^{-1}$, $N_m^{\text{Fe II}} \approx 10^{-2}N(\text{Fe II}) \approx 10^{-6}N_{\text{H}}$, $r_b \approx 0.5 \times 10^{15} \text{ cm}$, and $\Delta v_D^{m4} = 7 \times 10^{-6}v_0$ (for $T \approx 5000 \text{ K}$ for HI zone (Verner et al. 2002)) we get $\sigma_{m4} \approx 2.5 \times 10^{-14} \text{ cm}^2$ and $\tau_{m4} \approx 1.3 \times 10^{-7}N_{\text{H}}$. The magnitude of N_{H} cannot be

less than the critical value $N_{\text{cr}} = (0.5 \text{ to } 5) \times 10^7 \text{ cm}^{-3}$, as it is only in this case the cold HI zone of the blob and hence the narrow fluorescence lines are formed (Johansson & Letokhov 2001). Therefore, the optical density $\tau_{m4}(\text{Fe II}) \gtrsim 1\text{--}10$. Thus, the Ly α radiation from the stellar wind that is in exact resonance with the Fe II absorption line ensures a preferable excitation of the Fe⁺ ions in the outer shell of the blob. Even when $\tau_{m4} \approx 10\text{--}10^3$, excitation within the limits of $\pm 2\Delta\nu_{\text{D}}^{m4}$ detuning in the wings of the absorption line can also provide for the excitation of the Fe⁺ ions throughout the blob volume. However, the intensity of pumping radiation and hence the intensity of fluorescent lines should be larger in the outer shell, which is in agreement with observations (Smith et al. 2004).

Those wavelength bands of the stellar-wind Ly α profile, which are in resonance with the Fe II absorption lines (Fig. 2) are detuned substantially from the narrow hydrogen 1s-2p absorption line in the cold zone of the blob. However, they are subject to coherent scattering in the Lorentz wings of HI, as shown in Fig. 2. The scattering cross section is defined by the expression

$$\sigma_{\text{sc}}(\Delta\nu) = \frac{\Delta\nu_{\text{D}}^{\text{HI}} \delta\nu_{\text{rad}}}{(2\Delta\nu)^2} \sigma_{\text{sc}}^0, \quad (5)$$

where σ_{sc}^0 is the scattering cross section at the line center, $\Delta\nu_{\text{D}}^{\text{HI}}$ is the Doppler width of HI, $\delta\nu_{\text{rad}}$ is the radiative width of the 1s-2p transition that determines its Lorentzian profile, and $\Delta\nu$ is the detuning of the stellar wind H Ly α spectral band, which is in resonance with the Fe II absorption line. Consider as an example the case where $\Delta\nu \approx 160 \text{ cm}^{-1}$ ($\Delta\nu_{\text{D}}^{\text{HI}} = 2.4 \text{ cm}^{-1}$, $\delta\nu_{\text{rad}} = 2.5 \times 10^{-3} \text{ cm}^{-1}$). In that case, $\sigma_{\text{sc}}(\Delta\nu) \approx \sigma_{\text{sc}}^0 \cdot 6 \times 10^{-8}$, which for $\sigma_{\text{sc}}^0 = 1.4 \times 10^{-14} \text{ cm}^2$ yields $\sigma_{\text{sc}}(\Delta\nu) \approx 10^{-21} \text{ cm}^2$. Hence we have the following estimate for the coherent scattering length: $l_{\text{sc}} = 10^{21}/N_{\text{H}}$. Again at $N_{\text{H}} = (0.5 \text{ to } 5) \times 10^7 \text{ cm}^{-3}$ the coherent scattering length $l_{\text{sc}} \approx (0.2 \text{ to } 2) \times 10^{14} \text{ cm}$, i.e., it is less than the blob radius $r_{\text{b}} \approx 5 \times 10^{14} \text{ cm}$. Thus, the HI zone in the blob is a scattering medium for the Ly α photons that selectively excite the Fe⁺ ions. It takes about $N_{\text{sc}} \approx (r_{\text{b}}/l_{\text{sc}})^2 \approx 6\text{--}600$ scattering events for the photons to penetrate inside the blob. This situation is more favorable than that for the Ly α photons originating in the HII zone of the blob, since they have a more wide Doppler width: $\Delta\nu_{\text{D}}^{\text{HII}} \approx 10 \text{ cm}^{-1}$ and can be absorbed by HI more strongly.

Based on this simple picture of the basic photoprocesses occurring in the blob, we can state that the narrow spectral lines observed are formed all over the volume of the blob.

3. Observational setup and conditions

The observations presented in this paper are part of a campaign conducted at the Pico dos Dias Observatory (LNA/Brazil) using the Coudé focus of the 1.6-m telescope. The CCD was a Marconi 2048 × 4608 pixels and the slit width was 1.5 arcsec, resulting in a resolution of $R = 13\,000$ (2 pixels) at Balmer α , as measured using a thorium-argon lamp. Extractions of the spectrum were made in 5 rows along the spatial direction encompassing ~ 2.0 arcsec around the central star. Changing the number of extracted rows from 3 to 9 did not produce measurable

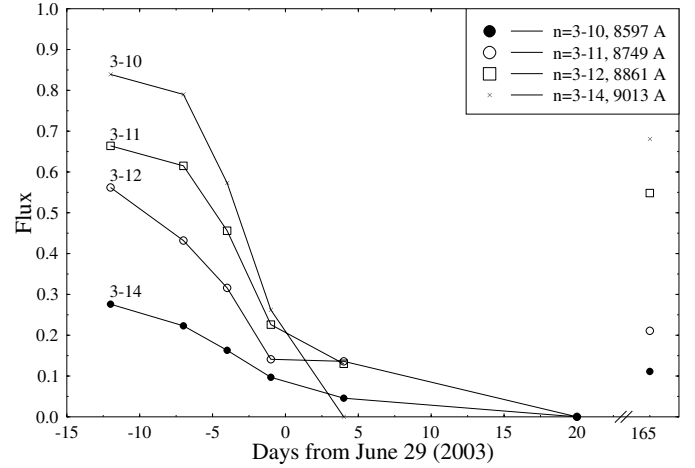


Fig. 4. Time behaviour of HI Paschen lines during the spectroscopic event.

changes in the line intensities. Also changes in the slit width in the range 1–3 arcsec produced no significant differences in the spectrum. This is important, because the seeing was variable along the observing program, especially in late July and early August, when the star is at large airmass in the beginning of the night. The largest impact on the repeatability of line intensities was caused by guiding errors, that occurred at large telescope inclinations. For wavelengths longer than 6500 Å, we observed also the neighbor bright star θ Car ($V = 2.6$, $\text{sp} = \text{B0V}$) in order to remove CCD fringing and telluric lines. The stellar continuum was normalized by fitting a low order polynomial.

The procedure to measure the equivalent width of the narrow line components was integrating the area under the line profile in the classical way. However, the narrow components are seated on broad components and in some cases, are blended with other lines that can be variable. To avoid the contamination of variations, we measured the equivalent widths of the narrow components referred to the normalized stellar continuum, not to the flux at the base of the narrow line components. The stellar continuum itself is variable, although only by a small amount in the spectral range we are interested.

4. Intensity variation of HI Paschen lines

In Fig. 4 we present data on the intensity variation of the HI Paschen lines (narrow components) from all the Weigelt blobs. The reduction of the intensities of the lines can be explained by the reduction of the ionizing radiation flux from the central source in Eta Carinae. This can take place if the recombination rate W_{rec} of the H ions in the hot HII zones of the Weigelt blobs is higher than the reduction rate of the ionizing radiation intensity. Otherwise the intensity of the recombination hydrogen lines $n \rightarrow 3$ would remain unchanged during the course of the spectral event. Note that the cold HI zones of the blobs cannot be the source of the Paschen lines.

From the curves in Fig. 4 we adopt that the intensity of the stellar radiation decreases by a factor of 2 during 3 days

which gives an estimate of the lower limit of the initial (prior to the spectral event) electron density, n_e in the HII zones of the Weigelt blobs:

$$W_{\text{rec}} = \alpha \cdot n_e \gtrsim (3 \times 10^5 \text{ s})^{-1}, \quad (6)$$

where $\alpha = \sum \alpha_n = 3 \times 10^{-11} / \sqrt{T_e} (\text{cm}^3 \text{s}^{-1})$ is the sum of the recombination coefficients for each level. From expression (6) we get $n_e \gtrsim 10^7 \text{ cm}^{-3}$ for $T_e \approx 10^4 \text{ K}$ in the HII zone. This estimate agrees quite well with the estimate of the critical hydrogen concentration N_{cr} in the blobs.

The relative intensities $I(\text{Pa}_n)$ of the HI Paschen lines depend on the corresponding recombination coefficients α_n and branching fraction from the upper level $BF(\text{Pa}_n)$:

$$I(\text{Pa}_n) \simeq BF(\text{Pa}_n) \alpha_n n_e(t) N_{\text{HII}}(t), \quad (7)$$

where $n_e(t)$ and $N_{\text{HII}}(t)$ are the time dependencies of the electron and ion concentrations during the reduction of the ionizing flux from the central source. The relative intensities of the Paschen lines in Fig. 4 are in qualitative agreement with expression (7). Actually, the difference in intensities of lines “3- n ” corresponds to the decrease of the recombination coefficient α_n with higher quantum number n . The temporal decrease of intensities for the lines corresponds to the reduction of the electron $n_e(t)$ and proton $N_{\text{HII}}(t)$ densities during the spectral event.

5. Intensity variations of Fe II fluorescence lines from highly excited states

Figure 5a displays the observed intensity observations for 12 spectral lines of Fe II excited by $\text{Ly}\alpha$ radiation. All these fluorescence lines correspond to the $5p \rightarrow 5s$ transition array (marked A in Fig. 3) in Fe II. The rate of intensity reduction of the fluorescence lines is approximately the same as that of the recombination Paschen lines (Fig. 4). This points to a common origin of the effect of reduction of the intensity of the spectral lines of interest. In the case of Paschen lines, the effect is associated with the decrease in the intensity of the Lyman continuum radiation, Ly_c , that sustains the ionization balance of the H II ions in the blobs, while in the case of (Fe II) lines, the effect is due to the reduction of the ionization balance in the stellar wind that emits the wideband $\text{Ly}\alpha^{\text{sw}}$ radiation (Fig. 2c).

The wavelength difference between the $\text{Ly}\alpha$ pumped Fe II lines, responsible for the occurrence of these 12 fluorescence lines, and $\text{Ly}\alpha$ itself ranges between -2.6 and $+2.5 \text{ \AA}$, as shown in Fig. 6. The plot shows the intensity of $\text{Ly}\alpha$ as indirectly measured from the observed intensity in the fluorescence lines, which is corrected for the branching fraction of the fluorescence line and for the oscillator strength of the excitation channel. The lower levels of all the excitation channels belong to the $(^5\text{D})4s \text{ a}^4\text{D } LS$ term, and no correction for different populations in the different fine-structure levels has been applied. Two sets of theoretical atomic data for Fe II, Kurucz (2001) and Raassen (2002), have been used to derive the $\text{Ly}\alpha$ intensities from the fluorescence lines. The resulting intensities are presented in Fig. 6 by crosses using atomic data from Kurucz (2001) and open circles using data from Raassen (2002).

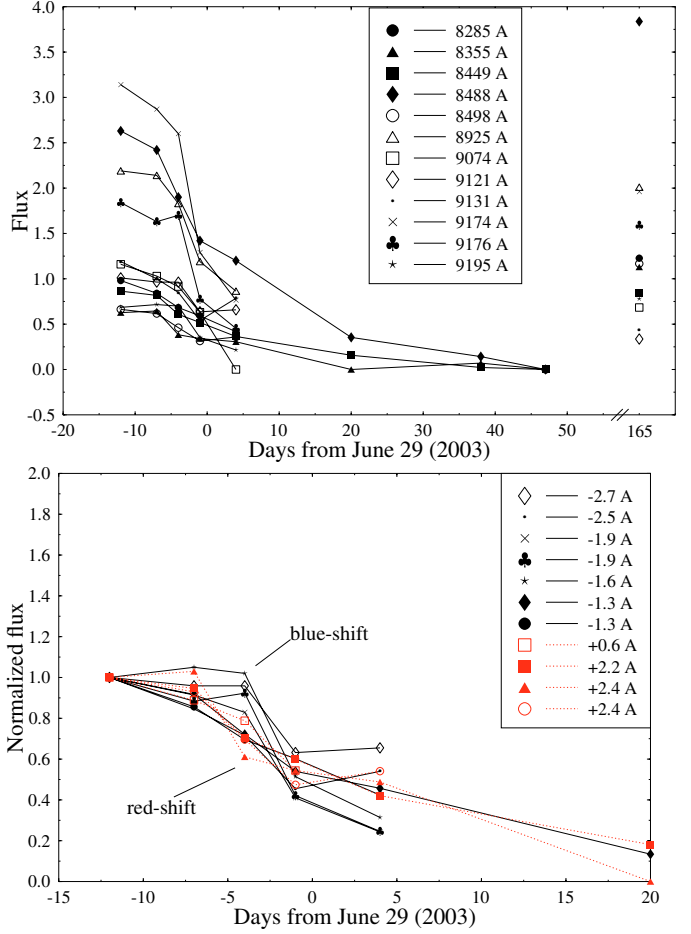


Fig. 5. a) Time behaviour of fluorescent (Fe II) lines during the spectroscopic event. All lines are $5p \rightarrow 5s$ transitions (A in Fig. 4). The wavelengths are indicated in the inserted key. All lines were not observed after the event. b) Same as a), but normalized to June 17 (–12 days). In the key, the wavelength detuning of each excitation channel from $\text{H}\text{Ly}\alpha$ is indicated. A positive value indicates a redshift. Note the different time scales.

The differences reflect the difficulties in calculating atomic parameters for complex spectra like Fe II. The two upper levels responsible for the excitation lines at 2.2 and 2.5 Å in Fig. 6 are known to be heavily mixed making the corresponding calculated f -values very uncertain. Based on laboratory intensities we have for either of the two levels divided the total line strengths in two equal parts both for the excitation channels and the fluorescence lines. This means that the excitation channels to the two upper levels are equally efficient, and that the resulting fluorescence lines to a given lower state has the same strength. The $\text{Ly}\alpha$ pumped Fe II states represented in Fig. 6 are excited by various parts of the wide $\text{Ly}\alpha^{\text{sw}}$ profile associated with the stellar wind (Fig. 2c). It should be emphasized that the width of the spectral interval ($\pm 2.5 \text{ \AA}$) corresponds to a terminal stellar wind velocity of $\pm 625 \text{ km s}^{-1}$ relative to the the motion of the Weigelt blobs.

During the spectral event there is a reduction in the intensity of the Ly_c radiation that ionizes both the blobs and the stellar wind (Fig. 1). As a result, the blobs become neutral with no frontal HII zone, and the Strömgren boundary in the stellar

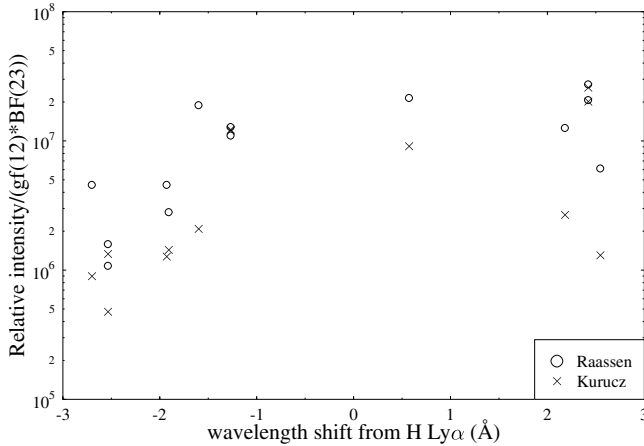


Fig. 6. Indirect measurement of the shape of the HLy α profile at 1215 Å. The intensity at a certain wavelength is derived from the strength of a fluorescence line, adjusted for the strength of the excitation channel and the branching fraction of the actual fluorescence line. Two different sets of atomic data were used: (x) from Kurucz (2001) and (o) from Raassen (2002). For the points at +2.2 and +2.5, which correspond to upper levels that are known to be mixed, the atomic parameters have been adjusted.

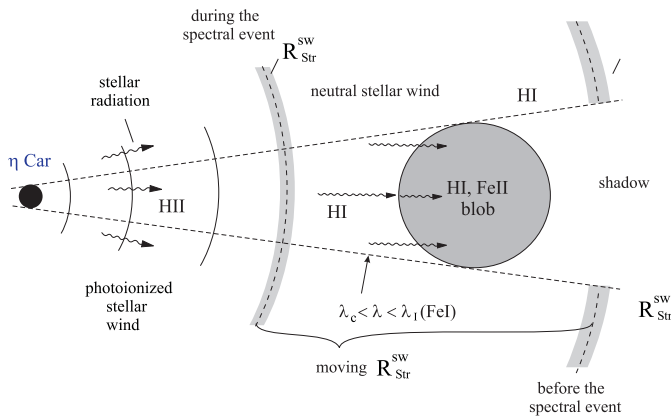


Fig. 7. Sketch of the motion of the Strömgren boundary in the stellar wind toward the central source in Eta Carinae during the spectral event.

wind, $R_{\text{Str}}^{\text{sw}}$, shifts toward the central source, as shown in Fig. 7. A somewhat faster reduction of the intensity of some of the $\langle \text{Fe II} \rangle$ fluorescence lines would be a confirmation of such a shift of the Strömgren boundary for the stellar wind, because their excitation requires the red-shifted part of the Ly α^{sw} profile, which originates from the back side of the Weigelt blobs.

To illustrate the time dependence of the intensity reduction in the fluorescence lines for various wavelength shifts of the Ly α radiation we have in Fig. 5b made normalized intensity reduction curves for the twelve $\langle \text{Fe II} \rangle$ fluorescence lines. The relative intensity change with time for each $\langle \text{Fe II} \rangle$ line shows that those lines, whose excitation requires the red-shifted part of Ly α^{sw} , tend to decay a few days sooner than the $\langle \text{Fe II} \rangle$ lines excited by the blue-shifted part. This fact is consistent with our model proposing that the pumped Fe II levels are mainly excited by the Ly α^{sw} radiation from the stellar wind, in which the

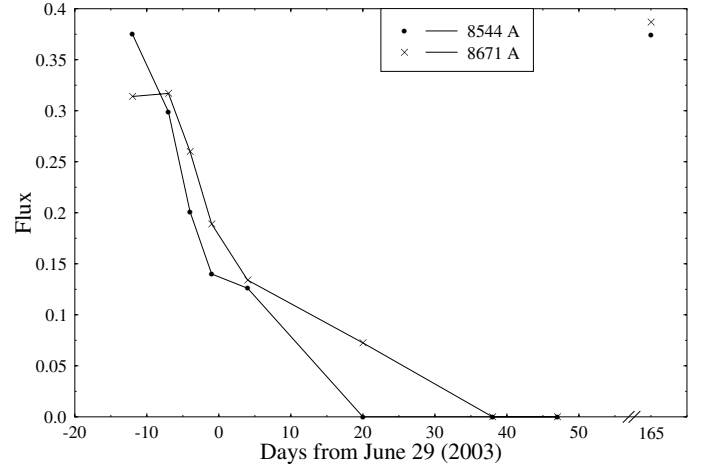


Fig. 8. Time behaviour of Fe II laser lines during the spectroscopic event. The lines are $4s^* \rightarrow 4p$ transitions (B in Fig. 3). Note the different flux scale compared to Fig. 5a.

Strömgren boundary is moving during the time of the spectral event (see also Johansson & Letokhov 2004b).

Variations of the intensity of two spectral lines corresponding to $4s^* \rightarrow 4p$ transitions (transitions B in Fig. 3) are also observed. In this case the fluorescent decay is from the pseudo-metastable states $4s^*$, which have long lifetimes in spite of their potential decay in LS -allowed transitions. These two fluorescence lines should exhibit a strong stimulated emission of radiation, since an inverted population is formed between the levels $4s^*$ and $4p$ (Johansson & Letokhov 2002, 2003, 2004b). The intensity variation character of these laser lines is similar to the behavior of the variation of the fluorescent $5p \rightarrow 5s$ transitions (transition A in Fig. 3) featuring neither population inversion, nor stimulated emission effects. This can be explained by the fact that the emission intensity in transitions A and B is limited by the rate of pumping by the Ly α radiation, why it follows the pattern of the intensity variation of the Ly α pumping line. The only difference is that the intensity of the laser lines in the slow transition B is comparable with that of the fluorescence lines in the fast allowed transition A, just because of stimulated emission of radiation under saturated amplification conditions (Johansson & Letokhov 2004b).

6. Intensity variations of forbidden Fe II lines from low-lying metastable states

We have also studied intensity variation curves for five forbidden [Fe II] lines due to transitions between low-lying metastable states, as illustrated in Fig. 9. Their time behavior differs substantially from that of the $\langle \text{Fe II} \rangle$ fluorescence lines associated with transitions between high-lying energy levels with short lifetimes. The shape of the curves in Fig. 9 can be explained by the fact that the contribution to the population of the metastable states comes from two excitation mechanisms. One is the radiative decay of the high-lying states excited by Ly α^{sw} . The efficiency of this channel changes during the period of a spectral event, because it depends on the Ly α^{sw} radiation and, in the final analysis, on the intensity of the stellar wind.

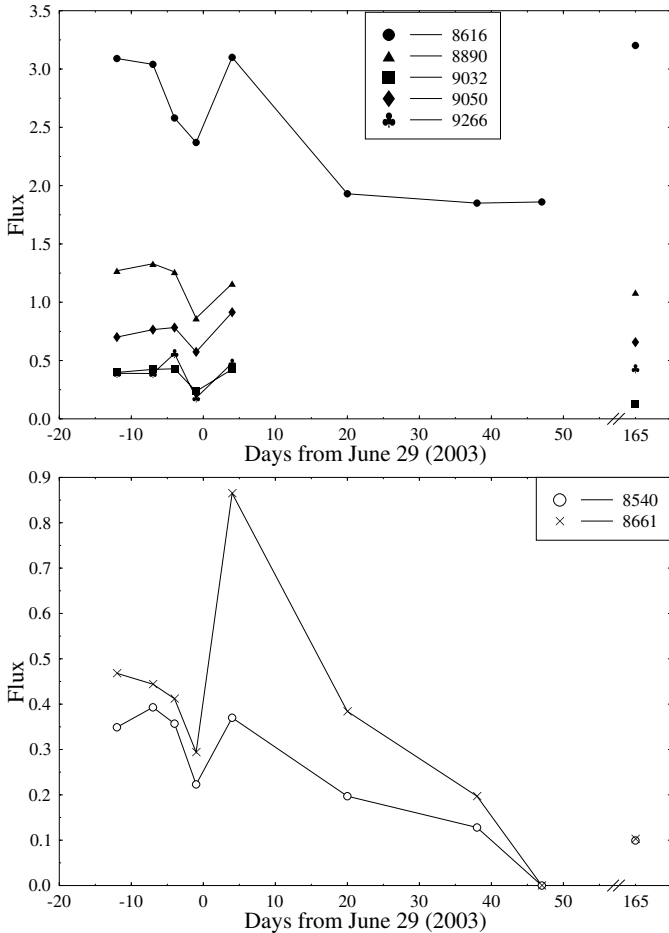


Fig. 9. a) Time behaviour of forbidden [Fe II] lines during the spectroscopic event. The lines belong to the multiplet $3d^7 a^4F-3d^7 a^4P$ (12F). Only the 8616 Å line was observed during the period after the event. Compare with the time behaviour of the fluorescent lines in Fig. 4. b) Same as a), but for Ca II $3d^2D-4p^2P$.

The other mechanism is the collisional electronic excitation. This channel depends on the concentration of electrons in the HI zone. Since this channel does not decay during the period from 22 June to 15 August or longer (50–100 days), the electron recombination rate $W_{\text{rec}} < 10^{-7} \text{ s}^{-1}$ and, according to Eq. (4), $n_e < 3 \times 10^4 \text{ cm}^{-3}$. This agrees well with the electron concentration in the HI zone, governed by the photoionization of the Fe atoms, i.e., $n_e \approx N(\text{Fe II}) \approx 10^3-10^4 \text{ cm}^{-3}$.

An amazing fact is the growth of the intensity of the forbidden [Fe II] lines in the first half of July, when the spectral event is at its minimum. This can, in principle, be explained by a temporary increase in the electron density n_e for unknown reasons. Moreover, this possibility is probably supported by the fact that the same temporary intensity increase is exhibited by two Ca II lines. These are also due to transitions between relatively low-lying levels that can be excited by electrons. Naturally the absence in Ca II of low-lying metastable states and transitions coincident with the $\text{Ly}\alpha$ radiation makes the intensity behavior of the Ca II lines different from that of the Fe II lines.

7. Conclusion

The results extracted from the extensive ground-based spectral observations of H and Fe II lines formed in the Weigelt blobs of Eta Carinae support and supplement the picture of the photo-physical processes taking place in the near vicinity of the central source. The Weigelt blobs provide essentially a sensitive probe for these photoprocesses, especially during the course of the periodic and temporary reduction of the stellar radiation intensity during the spectral event. So far, we do not know the true source of the photoionizing radiation. Most likely it is the combined radiation from the primary and secondary stars in a binary system. One can suppose that during the spectral event the radiation from the hotter secondary star is temporarily screened by the primary star as seen from the Weigelt blobs. This leads to the reduction of the intensity of the ionizing radiation reaching the blobs for a period of the order of 100 days.

As a first result of the reduction of the ionizing radiation, the Strömgren boundary R_{Str}^b disappears from the blobs, so that they become practically neutral. This manifests itself in the reduction of the intensity of the recombination Paschen lines from the HII zone of the blobs.

Secondly, the Strömgren boundary $R_{\text{Str}}^{\text{sw}}$ in the stellar wind moves closer to the central source. As a result, the red-shifted part of the $\text{Ly}\alpha^{\text{sw}}$ radiation disappears first and then the blue-shifted part. This is manifested in the behavior of the intensity reduction of the (Fe II) lines. For the time being we can only speak of this tendency for the consecutive change in the intensity of the (Fe II) lines, as we observe the total radiation in these lines from all the Weigelt blobs, which occupy somewhat different positions relative to the central source of Eta Carinae.

The reduced $\text{Ly}\alpha^{\text{sw}}$ radiation results in some reduction in the intensities of the forbidden [Fe II] lines from low-lying metastable states in Fe II. This is due to the decrease in the population of these states resulting from the fluorescence decays of high-lying states. The remaining part of the intensity in the [Fe II] lines is due to excitation by collisions with electrons. The low concentration of electrons in the HI zone prevents the Fe^+ ions from recombination throughout the three months duration of the spectral event.

Finally, the intensity variation of the Paschen lines, the fluorescence (Fe II) lines, and the forbidden [Fe II] lines make it possible to estimate the concentration of electrons in the HI and HII zones of the Weigelt blobs. These qualitative estimates agree with the theoretical values calculated earlier.

Acknowledgements. The research project is supported by a grant (S.J.) from the Swedish National Space Board. A.D. thank FAPESP and CNPq Brazilian agencies and to Lund University for support. V.S.L. acknowledges the financial support through grants (S.J.) from the Wenner-Gren Foundations, as well as Lund Observatory for hospitality, and the Russian Foundation for Basic Research (Grant No. 03-02-16377).

References

- Bautista, M. A., & Pradhan, A. K. 1998, *ApJ*, 492, 650
 Brown, A., Jordan, C., & Wilson, R. 1979, in *The first year of IUE*, ed. A. Willis, 232

- Damineli, A. 1996, *ApJ*, 460, L49
- Damineli, A., Conti, P. S., & Lopes, D. F. 1997, *New Astron.*, 2, 107
- Davidson, K. 2001, in *Astronomical Society of the Pacific Conf. Ser.*, 3
- Davidson, K., & Humphreys, R. M. 1997, *ARA&A*, 35, 1
- Davidson, K., Ebbets, D., Weigelt, G., et al. 1995, *AJ*, 109, 1784
- Davidson, K., Ebbets, D., Johansson, S., Morse, J. A., & Hamann, F. W. 1997, *AJ*, 113, 335
- Gull, T. R., Ishibashi, K., Davidson, K., & The Cycle 7 STIS Go Team 1999, in *Eta Carinae at the Millennium*, ed. J. A. Morse, R. M. Humphreys, & A. Damineli., *ASP Conf. Ser.*, 179, 144
- Gull, T., Ishibashi, K., Davidson, K., & Collins, N. 2001, in *Eta Carinae and Other Mysterious Stars: The Hidden Opportunities of Emission Spectroscopy*, *ASP Conf. Ser.*, 242, 391
- Gull, T. R., Vieira, G., Bruhweiler, F., et al. 2005, *ApJ*, 620, 442
- Johansson, S., & Hamann, F. 1993, *Physica Scripta*, T47, 157
- Johansson, S., & Jordan, C. 1984, *MNRAS*, 210, 239
- Johansson, S., & Letokhov, V. S. 2001, *A&A*, 378, 266
- Johansson, S., & Letokhov, V. S. 2002, *J. Exp. Theor. Phys. Lett.*, 75, 495
- Johansson, S., & Letokhov, V. S. 2003, *Phys. Rev. Lett.*, 90, 011101
- Johansson, S., & Letokhov, V. S. 2004a, *Astron. Lett.*, 30, 58
- Johansson, S., & Letokhov, V. S. 2004b, *A&A*, 428, 497
- Johansson, S., & Zethson, T. 1999, in *Astronomical Society of the Pacific Conf. Ser.*, 171
- Klimov, V., Johansson, S., & Letokhov, V. S. 2002, *A&A*, 385, 313
- Kurucz, R. 2001, <http://cfaku5.harvard.edu/atoms.html>
- Pittard, J. M., & Corcoran, M. F. 2002, *A&A*, 383, 636
- Raassen, A. J. J. 2002, <http://www.science.uva.nl/pub/orth/iron/>
- Smith, N., Morse, J. A., Gull, T. R., et al. 2004, *ApJ*, 605, 405
- Stahl, O., Weis, K., Bomans, D. J., et al. 2005, *A&A*, 435, 303
- Steiner, J. E., & Damineli, A. 2004, *ApJ*, 612, L133
- van Boekel, R., Kervella, P., Schöller, M., et al. 2003, *A&A*, 410, L37
- Verner, E. M., Gull, T. R., Bruhweiler, F., et al. 2002, *ApJ*, 581, 1154
- Weis, K., Stahl, O., Bomans, D. J., et al. 2005, *AJ*, 129, 1694